Optimization of Equipment Capacity and an Operational Method Based on Cost Analysis of a Fuel Cell Microgrid

Shin'ya OBARA
Kitami Institute of Technology, Power Engineering Lab., Dep. of Electrical and Electronic Engineering
Koen-cho 165, Kitami, Hokkaido 090-8507 Japan
obara@mail.kitami-it.ac.jp
phone/FAX +81-157-26-9262

Seizi WATANABE
Kushiro National College of Technology, Dep. of Mechanical Engineering
Otanozhike 2-32-1, Kushiro, Kokkaido 084-0916 Japan

Abstract

A microgrid requires a stable supply of electric power and heat, which is achieved by the cooperative operation of two or more pieces of equipment. The equipment capacity and the operational method of the equipment were optimized using a newly developed orthogonal array-GA (genetic algorithm) hybrid method for an independent microgrid accompanied by a fuel cell cascade system, solar water electrolysis, battery, and heat storage. This type of system had not been hardly developed until now. The objective function of the proposed system was the minimization of the total amount of equipment and fuel cost over ten years. For the first step in the proposed analysis method, the capacity of each piece of equipment and the operational method, which are considered to be close to the optimal solution of the system, are combined using the orthogonal array and factorial-effect chart, which are an experimental design technique. In the next step, the combination described above provides the initial values to the GA, and the GA searches for the optimal capacity and operational method for each piece of equipment in question. Compared with a simple GA, the convergence characteristic improves greatly using the proposed analysis method developed in this study.

Key Words: Numerical Simulation, Experimental Design, Orthogonal Array, Microgrid, Genetic Algorithm, Fuel Cell

1. Introduction

It is thought that the evolution of microgrids when using green energy reduces power transmission loss, makes the use of exhaust heat more effective, and promotes the utilization of green energy. However, to ensure a stable supply of electric power from the green energy powered microgrid, it is necessary to combine two or more types of energy generators. Therefore, operation of the microgrid requires consideration and cooperation between the pieces of energy equipment. Optimizing the operation technology for a compound energy system, which allows the energy equipment network to have various output characteristics, is important for the development of a clean microgrid [1-6]. Furthermore, the development of hydrogen-fueled microgrids using clean hydrogen energy is expected in the future [7-10]. Generally, because the input-output characteristics of energy equipment are nonlinear, it is necessary to solve a nonlinear multi-variable problem in the operational plan of a compound energy system. Technologies using a conjugate gradient method, integer programming, or genetic algorithm (GA) as an analysis method to address operation optimization of an energy system have been developed [11-14]. It is easy to introduce an analysis method using a simple GA to solve the multi-variable, nonlinear problem, and a GA can be easily adapted for a complex energy system [12]. However, when the analysis requires many variables with high accuracy, very long computational times are required due to the increase in the number of gene models that compose the chromosome model. Moreover, many semi-optimal solutions, which have values that are similar to the evaluation function (the adaptive value or the objective function) in an analysis of a complex problem, are obtained. The purpose of this study is to develop a computer algorithm for operational planning of a compound energy system with two or more design parameters with high precision based on cost analysis using a GA. Therefore, an orthogonal array and a factorial-effect chart [15-17], which are an experimental design technique, are introduced as a first step, and the capacity of and the operation method for each piece of equipment, which are considered to be close to the optimal solution for a compound energy system, are obtained. In the next step, after providing the capacity of each piece of equipment described above as initial values to the GA, the GA searches further for the capacity and the operational method for each piece of equipment. Using the two search steps described above and because the GA can search focusing on a set of equipment capacities and operational methods near the optimal solution, the optimal solution can be obtained more efficiently than when using the conventional method. The analysis method developed in this study is referred to as the orthogonal array-GA hybrid method and is described below. For the cost analysis of the fuel cell cascade, the microgrid, which consists of a complex fuel cell system with parameters that include a SOFC (solid-oxide fuel cell), a PEFC (proton-exchange membrane fuel cell), water electrolysis by photovoltaics, and a heat pump, the optimal

configuration, the equipment capacity and the operational method of the equipment, is investigated using the orthogonal array-GA hybrid analyzing method. Based on this investigation, the difference between the calculation time and analytic accuracy using a conventional GA and the proposed analysis method is clarified.

2. Configuration of Cascade Fuel Cell Microgrid

2.1 Outline of Microgrid Using Fuel Cell Cascade System

Figure 1 shows the concept for an independent microgrid powered by a fuel cell cascade system and green energy, which are discussed in this paper. This system comprises an electric power grid, a heat network (warm water), a SOFC, a PEFC, a steam reforming system, photovoltaics, a water electrolyzer, power conditioners (1) to (3), a heat pump, a hydrogen cylinder, an oxygen cylinder, a battery, and a heat storage tank. By supplying natural gas to the SOFC, alternating current electric power (200 V and 50 Hz are assumed) is output to the electric power grid from the power conditioner (1). The fuel used for the reformed gas is bio-methanol, and the heat source supplied to the reforming system is the exhaust heat from the SOFC or the combustion of the bio-methanol. By supplying the reformed gas to the PEFC, alternating current electric power is output to the electric power grid from power conditioner (1). The electric power from the photovoltaics is supplied to the electric power grid from the power conditioner (2) or to the water electrolyzer through a DC-DC converter. Furthermore, the electric power from the photovoltaics is stored in a battery or in the form of hydrogen and oxygen gas using water electrolysis. The heat output from the whole system is the exhaust heat from the SOFC, the PEFC, and the electric heat pump. Because the exhaust from the heat of the fuel cells is stored in the heat storage tank, heat can be supplied as demanded, with a time delay.

2.2 Configuration of the Reforming System

Figure 2 shows the details of the reforming system. The reforming system consists of an exhaust heat exchanger (HEX), a reforming unit (R/M), a shift unit (S/U), a condenser unit (C/S), and a CO oxidization unit (C/O). The R/M creates an endothermic reaction, and the S/U, C/S, and C/O create exothermic reactions. The R/M is heated when the high temperature exhaust gas from the SOFC or the combustion gas from the bio-methanol is supplied to the HEX. The reformed gas is stored in a cylinder after compression. The stored, reformed gas can be supplied to the PEFC at any arbitrary time. The exhaust heat from the SOFC and the PEFC is stored in the heat storage tank. When the amount of stored heat runs short due to the amount of heat demanded, an electric heat pump begins to operate.

The power consumption of the heat pump is covered with the power generated from the SOFC, PEFC, or photovoltaics.

3. Modeling of System

3.1 Cost Calculation of the System

Equation (1) is the cost calculation equation for a general energy system. Here, α_1, α_2, α_3, and α_4 in the formula are weighting factors, y_n is the operating period, C_m, C_n, C_k are the cost of power generating equipment, cost of the heat generating equipment, and the annual maintenance costs of the system, respectively. Moreover, θ_p and θ_h are the unit fuel prices for the generator and heat equipment, and f_m and f_n are the fuel consumptions. Therefore, the 1st term on the right side of Eq. (1) is equipment cost, the 2nd term is fuel cost, and the last term is maintenance cost. The 2nd term in the bracket in the 2nd term on the right side expresses the cost due to the environmental impact of the system, and φ_p and φ_h are the costs that accompany the discharge of greenhouse gases by the generator and heat equipment. The unit of each item is Japanese Yen (1 USD=78 JPY).

$$
\begin{aligned}
F_{obj} &= \alpha_1 \cdot \left(\sum_{m=1}^{M} C_m + \sum_{n=1}^{N} C_n \right) \\
&+ \sum_{mh=1}^{12} \left\{ \alpha_2 \cdot y_n \cdot \sum_{t=1}^{24} \left(\theta_p \cdot \sum_{m=1}^{M} f_{m,mh,t} + \theta_h \cdot \sum_{n=1}^{N} f_{n,mh,t} \right) + \alpha_3 \cdot y_n \cdot \sum_{t=1}^{24} \left(\varphi_p \cdot \sum_{m=1}^{M} f_{m,mh,t} + \varphi_h \cdot \sum_{n=1}^{N} f_{n,mh,t} \right) \right\} \\
&+ \alpha_4 \cdot y_n \cdot C_k
\end{aligned}
\tag{1}
$$

3.2 Inputs and Outputs from the System

The relationship between the input and the output between the electric power and the heat of an energy system is shown in Eqs. (2) and (3). The left sides of both equations supply terms for the electric power or the heat over the sampling time t, and the right side is the consumption of the electric power or heat. The 1st term on the right side of both formulas is a demand term for the electric power and heat. The left side of Eq. (2) assumes that the electric power is output by power generators, such as a fuel cells and photovoltaics, and M is the total number of power generators. Moreover, the left side of Eq. (3) is the output from the heat equipment, such as the heat pump and the exhaust of the fuel cell, and N is the total number of heat-producing pieces of equipment. The second terms on the right side of Eqs. (2) and (3) are the amount of electric power and heat consumed by equipment pieces I and J. The term describing the energy storage in the form of electricity and heat is included in the second term on the right side of each equation. The term that describes the

energy supplied from the electric discharge of a battery and the heat output from a heat storage tank is included on the left side.

$$\sum_{m=1}^{M} p_{m,t} = p_{needs,t} + \sum_{i=1}^{I} \Delta p_{i,t} \tag{2}$$

$$\sum_{n=1}^{N} h_{n,t} = h_{needs,t} + \sum_{j=1}^{J} \Delta h_{j,t} \tag{3}$$

3.3 Energy Balance and Characteristics of the Equipment

3.3.1 The Power and Heat Balance

Equations (4) and (5) are the energy balance formulas for the electric power and the heat of the independent microgrid, respectively, as shown in Fig. 1. The left side and the right side of each equation are the input and output terms, respectively. The variables $\Delta p_{needs,t}$ and $\Delta h_{needs,t}$ on the right side of each equation are the amount of electric power and heat demand from the system. The efficiency of each piece of equipment, except the battery and the heat storage tank, depends on the load factor. Moreover, the output from the photovoltaics is distributed and directly supplied to the power grid ($p_{pex,t}$), stored in a battery ($\Delta p_{btc,t}$), and supplied to the water electrolyzer ($\Delta p_{we,t}$) (Eqs. (6) to (8)). The exhaust heat from the SOFC is distributed to the heat network through the heat storage tank ($h_{hex,t}$) and to the reformer system ($\Delta h_{rm,t}$) (Eqs. (9) and (10)).

The variables $r_{pex,t}$ and $r_{hex,t}$ in Eqs. (6) through (10) are random numbers between 0 and 1. Moreover, δ and δ', in Eqs. (6) and (7), are operation selection switches for the system and have a value of 0 or 1. The distribution method for the electric power obtained by the photovoltaics is expressed below.

$$p_{sofc,t} + p_{pefc,t} + p_{btd,t} \cdot \varphi_{btd} + p_{pex,t} = \Delta p_{needs,t} + \Delta p_{hp,t} + \Delta p_{btc,t} \cdot \varphi_{btc} + \Delta p_{we,t} \tag{4}$$

$$h_{hex,t} + h_{pefc,t} + h_{hp,t} + h_{st,out,t} \cdot \varphi_{st,out} = \Delta h_{needs,t} + \Delta h_{rm,t} + \Delta h_{st,in,t} \cdot \varphi_{st,in} + \Delta h_{rad,t} \tag{5}$$

$$\Delta p_{btc,t} = \delta \cdot \left(r_{pex,t} \cdot p_{pv,t} \cdot \varphi_{pc(2)} \right) \tag{6}$$

$$\Delta p_{we,t} = \delta' \cdot \left(r_{pex,t} \cdot p_{pv,t} \cdot \varphi_{pc(3)} \right) \quad \text{(where } \delta' = 0 \text{ occurs when } \delta = 1,\ \delta' = 1 \text{ is when } \delta = 0\text{)} \tag{7}$$

$$p_{pex,t} = \left(1 - r_{pex,t}\right) \cdot p_{pv,t} \tag{8}$$

$$h_{hex,t} = r_{hex,t} \cdot h_{sofc,t} \tag{9}$$

$$\Delta h_{rm,t} = \left(1 - r_{hex,t}\right) \cdot h_{sofc,t} \tag{10}$$

3.3.2 Input-output Characteristics of the Equipment

(1) The fuel cell

The loss of power conditioner (1) is included in each output $p_{sofc,t}$ and $p_{pefc,t}$ for the SOFC and the PEFC over the sampling time t. Moreover, because the efficiency of the fuel cell $\varphi_{fc,t}$ is strongly dependent on the load factor $\eta_{fc,t}$ (which equals the output of the power generation divided by the capacity of the equipment), $\eta_{fc,t}$ is first calculated using Eq. (11). Here, C_{fc} is the equipment capacity of the fuel cell. Furthermore, the efficiency of the power generation of the fuel cell $\varphi_{fc,\eta_{fc,t}}$ can be obtained by calculating Eq. (12) using $\eta_{fc,t}$. Eq. (12) is an approximate expression of the input-output characteristics of the SOFC and the PEFC, and ς, τ, and υ are each coefficients of the approximate expression. Each coefficient in Eq. (12) is obtained from the output characteristics (from the SOFC and PEFC) (Fig. 3 (a)) for each type of fuel cell. The fuel consumption $F_{fc,t}$ of the fuel cell is obtained by providing $\varphi_{fc,\eta_{fc,t}}$ to Eq. (13).

$$\eta_{fc,t} = p_{fc,t} / C_{fc} \tag{11}$$

$$\varphi_{fc,\eta_{fc,t}} = \varsigma \cdot {\eta_{fc,t}}^2 + \tau \cdot \eta_{fc,t} + \upsilon \tag{12}$$

$$F_{fc,t} = p_{fc,t} / \varphi_{fc,t} \tag{13}$$

The heat output of the fuel cell $h_{fc,t}$ is calculated from the relationship between the exhaust heat output in each fuel cell in Fig. 3 (a) and $\eta_{fc,t}$, as shown in Eq. (14), where ξ, ψ, and ζ in Eq. (14) are each coefficients of the approximate expression.

$$h_{fc,t} = \xi \cdot {\eta_{fc,t}}^2 + \psi \cdot \eta_{fc,t} + \zeta \tag{14}$$

(2) The reforming system

The defining equation for reformer efficiency is shown in Fig. 3 (b). The performance of the R/M, S/U, and C/O is contained in the reformer efficiency, as shown in Fig. 3 (b). Equation (15) defines the reformer efficiency in this paper. The difference in the reformer efficiency divided by the difference in the load factor of the reforming system is at most 10%.

$$\varphi_{rm,t} = \frac{\text{Lower calorific value of the reformed gas produced between } t \text{ and } (t+1)}{\text{The natural-gas supply calorific power between } t \text{ and } (t+1)} \times 100 \quad (15)$$

(3) Electric power from the photovoltaics

When the area of the photovoltaics is given, the amount of direct current electric power $p_{pv,t}$ output between the sampling time t and $t+1$ is determined using the amount of insulation and the efficiency of the solar cell power generation. The electric power of the photovoltaics is distributed to $p_{pex,t}$, $\Delta p_{btc,t}$, and $\Delta p_{we,t}$, as described in Section 3.3.1. The distribution of the electric power supplied from the photovoltaics will be selected depending on one of three modes. These modes are directly supplied to the power grid, stored as electricity in a battery, and supplied to the water electrolyzer. δ and δ' in Eqs. (6) and (7) are the "switches" that indicate the mode change in this case. The mode that directly supplies power to the power grid or stores it as electricity in a battery is further distributed based on the quantity directly supplied to the power grid $r_{pex,t}$ and the quantity stored electricity in the battery $(1-r_{pex,t})$ where $r_{pex,t}$ is a random number.

4. Analysis Method

4.1 Operation Optimization of the System Using a GA

In this paper, the optimal solution for the capacity of the energy equipment in an independent microgrid with a cascade fuel cell. The operation method for every sampling time t for each representative day over the course of a month are obtained using a GA based on cost analysis. The analysis method using a GA can easily be adapted for an energy system with a multi-variable, nonlinear problem. However, if the number of genes increases because many design parameters are introduced into the analysis, a large increase in the analysis time or the generation of many semi-optimal solutions may occur. Therefore, in this study, an orthogonal array table and a factorial-effect chart, which are used to aid the experimental design, are used as the first step. Accordingly, the combinations that are considered to be close to the optimal solution for the capacity of the system equipment and the operational method of equipment are investigated using the experimental design (design parameter analysis referred to as experimental design). For the next step, combinations of system equipment (design parameters) considered to be close to the optimal solution, as described above, are given as initial values for the GA, and the GA further searches for the optimal planning. The analysis method described above is described as the orthogonal array-GA hybrid method.

4.2 The Chromosome Model

In this study, the capacity of each piece of energy equipment in the microgrid and the operational method of each piece of equipment for every sampling time t for each day over the course of a month are optimized. Consequently, as shown in Fig. 4, the chromosomes used for the GA define seven equipment capacities (Fig. 4 (a)) as well as the operational method of these seven pieces of equipment (Fig. 4 (b)). Although the equipment capacity does not change over the course of a year, the operational method and the type of equipment differ for each day over the course of a month. Moreover, the number of chromosome models is N_{cr}. No.1, No.2, … n_{cr}, …, N_{cr} in Figs. 4 (a) and (b) are defined by the individual of the GA. Therefore, the part enclosed by the broken lines in Figs. 4 (a) and (b) is the gene information for an individual piece of equipment.

(1) Expression of the equipment capacity

Gene groups (1) through (7) in the chromosome model shown in Fig. 4 (a) represent the capacity of the energy equipment. The gene groups $p_{n_{cr},m,t}$ and $h_{n_{cr},n,t}$, which represent the output from the power generator equipment m and the heat equipment n by the chromosome number (individual number) n_{cr}, respectively, express the gene model group with r bits and are designated by a 0 or a 1. The maximum outputs of equipment pieces m and n are $C_{m,\max}$ and $C_{n,\max}$, and the minimum outputs are $C_{m,\min}$ and $C_{n,\min}$. The value of the decimal number for the gene model expressed by the random value of 0 or 1 is set to $d_{chrom,m}$ and $d_{chrom,n}$, respectively. $p_{n_{cr},m,t}$ and $h_{n_{cr},n,t}$ are determined by the following equations, where in the analysis example presented in this paper, the chromosome model of the equipment capacity and the operational method was set to r =16.

$$p_{n_{cr},m,t} = C_{m,\min} + d_{chrom,m} \cdot \left(C_{m,\max} - C_{m,\min}\right) / 2^r \tag{16}$$

$$h_{n_{cr},n,t} = C_{n,\min} + d_{chrom,n} \cdot \left(C_{n,\max} - C_{n,\min}\right) / 2^r \tag{17}$$

(2) Expression of the operational method

The electricity demand $\Delta p_{needs,t}$ and the heat demand $\Delta h_{needs,t}$ over the sampling time t for each day over the course of a month are known, and $p_{m,t}$ and $h_{n,t}$ from Eqs. (2) and (3) are expressed by the chromosome model shown in Fig. 4 (b). The individual number n_{cr} from Fig. 4 (b) consists of outputs $p_{n_{cr},m,t}$, $h_{n_{cr},n,t}$ from the power generator equipment m and heat equipment n at time t. Here, m and n are the numbers from the power generator and heat equipment. A gene includes information about $p_{n_{cr},m,t}$ or $h_{n_{cr},n,t}$, and

the number of individual chromosomes is n_{cr}. The system operational method can be achieved by decoding this chromosome model.

4.3 Objective Function (Adaptive Value)

When setting the cost minimization of the energy system as an objective function (the adaptive value determined by the GA), it is good to optimize using Eq. (1). However, to evaluate the economical efficiency of the energy system simply, calculating of the payback period λ_{year}, shown in Eq. (18), is widely used. Here, θ_{conv} and f_{conv} are the unit prices and quantity of fuel that are consumed by the system, which are compared to the proposed system.

$$\lambda_{year} = \sum_{mh=1}^{12}\left[\sum_{t=1}^{24}\left\{\theta_{conv}\cdot f_{conv,mh,t} - \left(\theta_p \cdot \sum_{m=1}^{M} f_{m,mh,t} + \theta_h \cdot \sum_{n=1}^{N} f_{n,mh,t}\right)\right\}\right] \Bigg/ \left(\sum_{m=1}^{M} C_m + \sum_{n=1}^{N} C_n\right) \tag{18}$$

However, energy systems continue to diversify, and the limitations of common systems are more difficult to address than those of the current system. Therefore, in this study, the cost of system equipment and the fuel charge for ten years (Eq. (19)) are used as the objective function. The fuel charge for ten years is used because there is no economic desire for a system whose maximum payback period exceeds ten years.

$$F_{obj} = \alpha_1 \cdot \left(\sum_{m=1}^{M} C_m + \sum_{n=1}^{N} C_n\right) + \sum_{mh=1}^{12}\left\{\alpha_2 \cdot \lambda \cdot \sum_{t=1}^{24}\left(\theta_p \cdot \sum_{m=1}^{M} f_{m,mh,t} + \theta_h \cdot \sum_{n=1}^{N} f_{n,mh,t}\right)\right\} \tag{19}$$

Here, α_1 and α_2 in the above equation are 1.0; λ is set for ten years; each value of C_m and C_n and θ_p and θ_h are described in more detail in Section 6.3.

4.4 Method of Optimization and Analysis Flow

4.4.1 Method of Optimization

Although energy equipment capacity and the operational method for each piece of equipment are optimized using the GA, this paper examines the following three methods.

(1) Optimization of the general GA

Both the equipment capacity and the operational method are analyzed simultaneously by the GA.

(2) Subdivision of the equipment capacity analysis by repeating the calculations using the GA.

The GA is introduced for all combinations of the subdivided equipment capacity.

(3) Using the proposed method (orthogonal array-GA hybrid analysis)

The system equipment capacity is given as a design parameter for the orthogonal array for use with the experimental design. With the combination of equipment capacities determined by the orthogonal array, the optimization of the operational method is analyzed using the GA. Next, the factorial-effect chart for the experimental design is produced using the value of the objective function (the adaptive value) and combined with the equipment capacities determined by the orthogonal array, as described above. The combination of the system's equipment capacities are obtained and are considered to be close to the optimal solution based on the factorial-effect chart . The combination of capacities described above is passed to the GA as a set of initial values. Moreover, the optimization of equipment capacity and the operational method of each piece equipment are simulated in detail.

According to method (1) in the list above, when the amount of equipment increases, the number of trial iterations increases dramatically. Moreover, when a lot of equipment and several equipment capacities divisions are possible, and this information is used in method (2), the number of trial iterations increase substantially. Because method (3) limits the search range of the GA by introducing the technique of experimental design, it is expected that the optimal solution will be obtained with a small number of trial iterations.

4.4.2 Analysis Flow

The analysis flow for optimization methods (2) and (3) described in Section 4.4.1 is shown in Figs. 5 and 6, respectively.

(1) Method to repeat the GA for the subdivided equipment capacity (Fig. 5)

The red blocks are the part of the iteration calculated by subdividing the equipment capacity, and the other blocks are the same as the analysis flow from general GA. The capacity of each piece of energy equipment, which is set as the design parameter in parts (c) and (d), is divided and calculated repeatedly for the different combinations of capacity division for each piece of equipment; this analysis differs from the analysis method using general GA that is described in (1). Therefore, the chromosome model (Fig. 4 (a)) showing the equipment capacity is not used in method (2). Because the capacity of each piece of equipment is determined using parts (c) and (d), the equipment cost of each piece of equipment can be determined by multiplying these capacities by the unit price of the equipment (part (e)). After this, the calculation flow is the same as in general GA.

(2) Proposed method (orthogonal array-GA hybrid analysis, Fig. 6)

The red blocks are calculated from the orthogonal array based on the experimental design, and the other blocks are the same as those in the analysis flow using the general GA, as shown in the general GA. For the analysis method using the general GA, the investigation of the parameter analysis using experimental design is added to the beginning of the analysis (parts (b) through (e)). The parameter analysis of the experimental design can analyze the optimal solution using a small number of experimental iterations and without conducting an exhaustive search of the parameters. Consequently, the proposed method determines the combination of equipment capacity at the beginning (parts (b) through (e)) of the analysis based on orthogonal array, and this method searches for the optimal operation method using the GA for the combination of equipment capacities. Next, the adaptive value (Eq. (19)) is calculated based on the equipment capacity and the operational method, which was obtained based on the orthogonal array, and a factorial-effect chart is produced from these results. By analyzing the factorial-effect chart, the combination of the equipment capacity considered to be close to the optimal solution can be determined. Next, the combination of the equipment capacities described above is set as the initial values for the general GA. As a result, the optimal solution for the capacity of each piece of equipment and the operational method can be obtained using a very small number of iterations.

5. Orthogonal Array-GA Hybrid Analysis

5.1 Reduction in the Number of Trials Using Experimental Design

The experimental design is designed to determine the effect of each design parameter efficiently without trying all possible combinations of the design parameters by introducing the orthogonal array [15-17]. There are no correlations between the design parameters in the rows of the orthogonal array. Accordingly, the combinations of the value levels used in the orthogonal array are arranged such that the relationship between the design parameters is perpendicularly orthogonal (independent). Therefore, the total of each row of the orthogonal array can be used to estimate the effect of each design parameter independently. When the orthogonal array is introduced, the number of trials can be substantially reduced when combining all of the design parameters. For example, there are eight design parameters, and each design parameter can take one of two values (value level). Moreover, the remaining seven design parameters can be set three design values. The number of trial times for the exhaustive search in this case is $2^1 \times 3^7 = 4374$. However, there are many types of orthogonal arrays used in the experimental design. For example, when an L_{18} orthogonal array (Table 1) is used, 18 iterations ($e1$ to $e18$) are used with eight design parameters ((A) to (H) in Table 1)).

5.2 Orthogonal Array-GA Hybrid Analysis

Although numbers one to three are described in the orthogonal array shown in Table 1, these values indicate the levels of the design parameter. Moreover, Table 2 is a level table, which describes the value x from each level of parameter 1 to parameter 8 (the first level, the 2nd level, and the 3rd level). It is necessary to produce the level table beforehand. For example, when deciding each value level $x_{p2,1}$, $x_{p2,2}$, and $x_{p2,3}$ for parameter 2, the minimum and the maximum values that are permitted by parameter 2 are set to $x_{p2,1}$ and $x_{p2,3}$, respectively, and the mean value is set as $x_{p2,2}$. Next, the evaluation values f_{ek} (k =1, 2, ⋯, 18) for experiments $e1$ through $e18$ are calculated using Eq. (20) and the level value (Table 2) for each design parameter (A) through (H) in the orthogonal array (Table 1).

$$f_{ek} = P_{ek} + y_n \cdot \sum_{m=1}^{12} \sum_{t=0}^{23} f_{ek,t} = P_{ek} + y_n \cdot \sum_{m=1}^{12} \sum_{t=0}^{23} \left(\sum_{m=1}^{M} f_{m,t} + \sum_{n=1}^{N} f_{n,t} \right) \tag{20}$$

5.3 Determining the Initial Values for the GA Using the Factorial-Effect Chart

The average evaluation value for the value level ls for design-parameter pl is set to $\overline{f_{pr,ls}}$. For example, the average evaluation value $\overline{f_{(B),2}}$ for the 2nd level of the design parameter (B) is an average of the evaluation values f_{e4}, f_{e5}, f_{e6}, f_{e13}, f_{e14}, and f_{e15} for experiment numbers $e4$, $e5$, $e6$, $e13$, $e14$, and $e15$, as shown in Table 1. The factorial-effect chart shown in Fig. 7 is an example that was taken from this result. When the objective function is filled such that the value of $\overline{f_{pr,ls}}$ is small, this level is considered to be close to the optimal solution for each design parameter (A) through (H), and these levels are the white circles in Fig. 7.

The value level that is considered to be close to the optimal solution described above is s the largest level value for the effect. In the case of Fig. 7, it is thought that the design parameters (A) and (B) are optimal at the 2nd level (namely, near the mean value), as shown in Table 2. For (C), (D), (F), and (G), the optimal solution is the 3rd level (namely, near the maximum), and for (E) and (H), the optimal solution is the 1st level (namely, near the minimum). In this paper, each large value level of the effect described above is given as an initial value to the GA. As a result, the efficiency of the analysis is expected to improve substantially because the search range of the GA is focused near the optimum value.

6. Analysis Conditions

6.1 Outline of the System

The cascade fuel cell microgrid described in Section 2 is introduced in Sapporo, Japan (cold, snowy area), and the optimization of a system that supplies electric power and heat to 30 average residences is investigated. Figure 8 (a) shows the load pattern of the microgrid [18]. An electric light and a household appliance are contained in the power load and are shown in Fig. 8 (a). Furthermore, a load with a hot-water space heater, water heater, and a bathtub are included in the heat load (Fig. 8 (b)). The load for cooling in the summer is not used for common residences in Sapporo.

6.2 Determining the Level of the Design Parameters

It is necessary to choose the type of orthogonal array described in Section 5 given the number of design parameters and the number of levels introduced into the orthogonal array. Orthogonal arrays, such as L_4, L_8, L_{16}, L_{32}, L_{64}, L_{128}, and L_{256}, are generally used when using two levels, and orthogonal arrays such as L_9, L_{27}, L_{81}, and L_{243} are generally used when using three levels. Moreover, the number of levels is mixed in L_{18} and L_{36} arrays. An orthogonal array with two levels is convenient for equipment that is ON or OFF. An orthogonal array for numbers with more than three levels can be produced. In the example analysis, seven design parameters, (A) through (G), are set and shown in Table 3. As shown in Table 3, two levels are defined for the solar cell, and three levels are defined for the other equipment. The design parameters (B), (E), (F), and (G) are the capacities C_{bt} of the battery, C_{fc} the fuel cell, C_{st} the heat storage tank, and C_{hp} the heat pump, respectively. The heat storage tank parameter is set to its minimum level 0 (heat storage is not carried out) (the 1st level). Moreover, the 1st level of E_{btd}, the electric discharge of the battery, and the E_{btc}, the charge of the battery, are also set to 0. From the number of design parameters and the number of levels, an L_{18} orthogonal array, as shown in Table 1, is used in this analysis. As a design parameter, the capacity of each piece of equipment, the amount of electric discharge from the battery E_{btd}, and the amount of battery charge E_{btc} were set. The maximum (the 3rd level) capacity C_{pv} of a solar cell can be 100 kW assuming it has the ability to fully provide the electric power of a residence as well as sustain the heat load in winter. The design parameters (A) were set at two levels based on the distribution of the electric power by the photovoltaics (Section 3.3.2 (3)). For the maximum of each design parameter, it was determined taking into consideration of the maximum quantity of the power and heat load.

6.3 Analysis Conditions

(1) Efficiency of the equipment

The efficiency of each piece of equipment used in the analysis is shown in Table 4. In this analysis, the loss of the power and the heat grid are not considered.

(2) The objective function of the system

The objective function is considered the minimum (Eq. (19)) of the sum total the equipment cost and the fuel consumption cost over ten years. C_m and C_n in Eq. (20) are calculated using Eqs. (21) and (22), respectively. Here, $p_{\max,m}$ and $h_{\max,n}$ are the maximum output (capacity) of the generator m and the heat equipment n, respectively. Moreover, the equipment unit prices u_m and u_n use each value in Table 5. The unit prices in Table 5 are determined by referring to the present equipment cost in Japan. The unit price of natural gas is 17.73 Yen/kWh, and the unit price of bio-methanol is 4.5 Yen/kWh. Natural gas is supplied to the SOFC, and the bio-methanol is used for the reforming fuel for the reforming system as well as the heat source for the reforming unit.

$$C_m = u_m \cdot p_{\max,m} \tag{21}$$

$$C_m = u_n \cdot h_{\max,n} \tag{22}$$

(3) The preparation of the orthogonal array and factorial-effect chart

Table 6 (a) shows the results from every value level for each design parameter obtained from the L_{18} orthogonal array, which is shown in Table 1, using the value level of each design parameter shown in Table 3. Accordingly, Table 6 (a) shows both the average equipment cost at each value level for each design parameter (A) through (H) and the fuel consumption over ten years. Moreover, Figure 9 (a) shows the analysis result from the L_{18} orthogonal array (rightmost row in the table), which is shown in Table 1. The operation method of the system was not found for $e1$, $e6$, $e7$, $e10$, $e11$, and $e14$, as shown in Fig. 9 (a) because there was a small output from the fuel cell, as shown in Table 3 for example, and enough output from the heat pump in the winter is not obtained. However, the equipment cost is obtained using Eqs. (21) and (22) if each design parameter from Table 3 is used.

However, when the combination of design parameters is not suitable because the operating method of the system is not obtained, the fuel cost cannot be calculated. Thus, the average values from other results were used to calculate the fuel cost for $e6$, $e7$, $e11$, and $e14$, but not $e1$ and $e10$, in this study. Because the combination of the values for the design parameters near the optimal solution found using experimental design are not suitable, the analysis time of for the next GA is long. If the accuracy of the initial values of the GA determined by the orthogonal array and the factorial-effect chart are poor, then the number of iterations for optimization by the next GA increases. However, even if the accuracy of the

initial values of the GA obtained from the orthogonal array and the factorial-effect chart is poor, the GA can search for the optimal solution.

(4) Determining the initial values for the GA

The red figures in Table 6 (a) show the minimum of the results calculated for each level and every design parameter. The results from the first level are the smallest for all the design parameters except for the capacity of the photovoltaics, which is design parameter (D) in Table 6 (a). Therefore, as initial values for the equipment capacity for the optimizing calculations performed by the GA, the first level in Table 3 is simply introduced as the starting value for each parameter (the capacity of photovoltaics is set to the second level). However, to determine more suitable initial values for the GA, the following rules were set up for this study:

a. When the combination of equipment capacities determined by the initial values for the GA clearly runs short of the electricity or heat demanded, increase the capacity of the fuel cells or the heat pump gradually according to each value level of the design parameters (Table 3).

b. For example, when electric power is insufficient, it is necessary to increase the output from the fuel cells or increase the capacity of the solar cell and the battery. The capacity of the SOFC (design parameter (B)) or the PEFC (design parameter (C)) can be increased to increase the output of the fuel cells. There are many combinations for the initial value of the GA, like the first level of the SOFC, the first level of the PEFC, the second level of the SOFC or the first level of the PEFC, the first level of the SOFC and the second level of the PEFC, or the first level of the SOFC and the 3rd level of the PEFC; the combination with the smallest level values are given in Table 6 (a).

c. Remove the combinations of design parameters that are clearly incompatible. The red figures in Table 6 (b) are each a value level for the design parameters that are determined to be initial values for the GA based on rules a. through c.. Because the level of the battery (design parameter (F)) and water electrolyzer (design parameter (H)) is 1 (capacity is zero), as shown in Table 6 (b), the solar cell should not be installed. Thus, the value level for design parameter (D) is set to the first level.

(5) Parameter Analysis of the GA

The generation number and chromosome number of the GA are set to 100 and 1000, respectively. The cross over probability $P_{r,cro}$ and mutation probability $P_{r,mut}$ were made into variables. Two kinds of chromosome models, the equipment capacity model (Fig. 4 (a)) and the operational method model (Fig. 4 (b)), are used in the analysis program. The probability of cross over and mutation is given for every chromosome group (Figs. 4 (a) and (b)) for the equipment capacity and the operational method ($P_{r,cro,eq}$, $P_{r,cro,om}$, $P_{r,mut,eq}$, $P_{r,mut,om}$).

7. Analysis Results

7.1 Convergence Characteristics and Equipment Configurations

Figure 10 (a) shows the analysis results obtained from the conventional GA and the analysis results including the generation number and the adaptive value (Eq. (19)) from the orthogonal array-GA hybrid method. Because each equipment capacity and the operational methods are made into the variables, as shown in Fig. 10 (a), it is very hard for the optimization analysis to converge using a simple GA. However, in the analysis completed by the orthogonal array-GA hybrid analyzing method proposed in this study and shown in Fig. 10 (b), convergence is achieved within 100 generations. The convergence values of each analysis shown in Fig. 10 (b) are in agreement as well.

In optimization by cost analysis using a cascade fuel cell microgrid with green energy, as shown in Fig. 1, the sum of the equipment and fuel cost for ten years is 4.42×10^8 Yen, as shown in Fig. 10 (b). The cost of the equipment is 3.53×10^8 Yen, and the fuel cost for ten years is 0.89×10^8 Yen. Currently, the equipment cost is very expensive compared to the fuel cost. As a result, the cascade fuel cell system, which uses the exhaust heat from the SOFC, is the major contributor to the equipment cost, as shown in Table 5, and is costly. Furthermore, operating the water electrolyzer using the electric power of the photovoltaics is also economically disadvantageous. If the discharge of greenhouse gas is considered, the optimal equipment configuration may differ from analysis results. According to the cost analysis in this study, a very simple system is more advantageous. Because the unit cost for each piece of equipment shown in Table 5 changes under various conditions, the system configuration is not easily determined.

Although the selection of the solution parameters from the GA requires some trial and error, the orthogonal array-GA hybrid method converges on the same values. Moreover, the method effectively increases the design parameters and the number of genes in an individual trial (chromosome model) by appropriately changing the type of orthogonal array, and this change improves the accuracy of the results. Therefore, the orthogonal array-GA hybrid method is a technique that can improve operational analysis over that using a conventional, simple GA.

7.2 Annual Operation Method

Figure 11 (a) shows the analysis results for the operational method of the PEFC, and Fig. 11 (b) shows the analysis results from the operational method of heat equipment (heat pump, heat storage tank, and exhaust heat of the PEFC). A lot of electric power is supplied to the heat pump by the heat load pattern given in Fig. 8 (a) because there is significant demand

for heat in the winter. As a result, the period excluding June to September has a lot of electricity production from the PEFC. However, an analysis of the maximum electricity production in June through September far exceeds the power load. Because the load factor for the heat pump in the summer is very small, operation of the heat pump becomes costly. Instead of operating the heat pump, the system operation is designed such that heat demand may be fulfilled by the exhaust heat and heat storage from the PEFC. Therefore, as shown in Fig. 11 (b), the exhaust heat output from the PEFC is almost the same throughout the year; the input and output from the heat storage tank are frequent in the summer. If the system is introduced into an area with a large heat demand, because the heat load in winter is larger than the power load, the operation of the system in summer primarily uses thermal power.

7.3 Equipment Capacity and the Optimal Configuration of the System

The red figures in Fig. 9 (b) are the results from the analysis of the optimal capacity of each piece of equipment using the orthogonal array-GA hybrid method proposed in this study. Furthermore, Fig. 12 shows the optimal configuration of the system determined from the results of Fig. 9 (b). The equipment configuration expressed above is the result of minimizing the cost using the equipment unit costs shown in Table 5, and the cost of the environmental impact and maintenance is considered. If an environmental impact term is added to Eq. (19), the objective function, the optimal configuration of the system may change substantially.

7.4 Comparison to the Conventional Energy Supply Method

The annual power and heat consumption for an average single-family house in Sapporo are 4,100 kWh and 25,300 kWh, respectively. Because many average residences utilize kerosene boilers, the heat source for a residence is conventionally assumed to be kerosene. The power rates for one residence in September, 2011 are 7,250 Yen/(month･house), and the monthly electric charge is 651 Yen/(month･house), and when a kerosene unit (at a cost of 98.3 Yen /L) is used, the energy consumption cost for a single-family home is 331,400 Yen/year (electric power 87,000 Yen and kerosene 244,400 Yen). Furthermore, the price for a kerosene boiler in Japan is 350,000 Yen (sum of the boiler, the kerosene tank, and the installation expense). When the cost of the boiler equipment and the fuel charge for ten years are added, the price is about 3,660,000 Yen/house. Therefore, the cost of the equipment and the fuel charge for the energy equipment for an average of 30 residences in Sapporo is 1.10×10^8 Yen in total. However, the sum for the equipment and fuel cost for 30 single-family

homes for ten years using the microgrid described in this paper is 4.42×10^8 Yen. Therefore, the cost of the system optimized in this paper is about 4 times the present energy cost.

8. Conclusions

In this study, the optimal configuration, the equipment capacity, and the operational method based on a cost analysis were investigated using numerical analysis and an independent microgrid, which introduced a cascade fuel cell system and a water electrolyzer by photovoltaics. Because the electricity and heat storage equipment were included on the proposed microgrid, the dynamic optimization problem with multiple variables using a GA (genetic algorithm) was discussed. It is easy to introduce a simple GA into this multi-variable, nonlinear problem. However, if a simple GA is used, as the number of variables increase and improvements in analytic accuracy are expected, a very long calculation time is required. Furthermore, many semi-optimal solutions are obtained from the analysis using a simple GA. Accordingly, in this study, the orthogonal array-GA hybrid method was developed. In this method, the equipment capacity and operational method, which are considered to be close to the optimal solution of the proposed system, are combined using an orthogonal array and a factorial-effect chart, which are known as the technique of experimental design. Next, the capacity of each piece of equipment expressed above is given as an initial value to the GA, and the GA searches for the capacities and the operational method for each piece of equipment. As a result, the orthogonal array-GA hybrid method developed in this study has good convergence characteristics compared to those of the simple GA, and one can expect that this method can be extended to complex energy systems because of its ability to respond to an increase in the number of genes.

The equipment capacity and the operational methods are optimized by the orthogonal array-GA hybrid method from the independent microgrid accompanied by a fuel cell cascade system, solar water electrolysis, accumulation of electricity, and heat storage. Operation of the microgrid for 30 single-family homes is optimized by minimizing cost (the sum total of equipment cost and the fuel cost for ten years) using the pattern of electricity and heat demand from a typical house in Sapporo, Japan. The equipment unit costs and unit fuel price are assumed to be the present values in Japan. As a result, the following conclusions are obtained.

(1) Steam reforming from the bio-methanol exhaust heat using the SOFC (cascade fuel cell system) and using the water electrolyzer powered by the photovoltaics is not cost-effective. The optimal system is a simple configuration using a methanol steam reformer, a PEFC, a power conditioner, a battery, a heat pump, and a heat storage tank.

(2) The sum of equipment cost and the fuel cost for ten years is 4.42×10^8 Yen. The cost of equipment is 3.53×10^8 Yen, and the remaining 0.89×10^8 Yen is the fuel cost for ten years. However, the sum of the purchased commercial electric power, the cost of equipment for 30 average single-family houses using a kerosene boiler, and the fuel charge for ten years is 1.10×10^8 Yen. If the environmental impact and other costs, which are not taken into consideration in this paper, are added to the objective function of the proposed system, the configuration of the system may change.

(4) The operational method of the proposed system was clarified after use for one year. Moreover, when the proposed system was introduced into an area with high heat demand, the priority operation of thermal power was planned throughout the year.

Acknowledgements

We received support for this research from the National Institute of Polar Research of Japan. We greatly appreciate the support of this foundation.

Nomenclature

C	Expense [Yen]
C_{bt}	Capacity of the battery [kWh]
C_{fc}	Capacity of the fuel cell [kW]
C_{hp}	Capacity of the heat pump [kW]
C_k	Annual maintenance cost of the system [Yen]
C_m	Maximum output of equipment m [kW]
C_n	Maximum output of equipment n [kW]
C_{pv}	Capacity of the solar cell [kW]
C_{st}	Capacity of the heat storage tank [kWh]
d_{chrom}	Value of the decimal number of the gene model
E	Electric power [kW]
E_{btc}	Amount of charge in the battery [kW]
E_{btd}	Amount of electric discharge from the battery [kW]
e	Experiment number
F_{fc}	Fuel consumption of the fuel cell [kWh]
F_{obj}	Objective function [Yen]
f	Fuel consumption [kWh]
f_{conv}	Fuel consumption of a comparable system [kWh]
f_{ek}	Evaluation value for the orthogonal array [kWh]
$\overline{f_{pr,ls}}$	Average evaluation value [kWh]
h	Heat [kW]

Δh	Exhaust heat from the SOFC supplied to a heat grid and a heat storage tank
I	Heat consumption [kW]
J	Amount of exhaust heat from the SOFC supplied to the reforming system
M	Number of pieces of equipment that consume electric power
N	Number of pieces of equipment that consume heat
N_{cr}	Number of pieces of generator equipment
n_{cr}	Number of pieces of heat equipment
p	Number of chromosomes
Δp	Electric power consumption [kW]
Δp_{btc}	Electric power of the solar cell stored in the battery [kW]
Δp_{we}	Electric power of the solar cell supplied to the water electrolyzer [kW]
r_{hex}	Random number between 0 and 1 (Eq. (9))
r_{pex}	Random number between 0 and 1 (Eq. (6))
t	Sampling time [Hour]
u	Unit price of the equipment [Yen/kW]
x_p	Value level [kW]
y_n	Operating period [Year]

Greek characters

α	Weight coefficient
δ, δ'	Value of 0 or 1 ($\delta'=1$ in the case of $\delta=0$, $\delta'=0$ in the case of $\delta=1$)
φ	Efficiency [%]
φ_h , φ_p	Cost of greenhouse gas emission [Yen]
η	Load factor [%]
λ_{year}	Payback period [Year]
θ_{conv}	Unit fuel price for the comparable system [Yen/kWh]
θ_p	Unit fuel price for the power generator [Yen/kWh]
θ_h	Unit fuel price for the heat equipment [Yen/kWh]
ξ, τ, υ	Coefficient for the approximate expression (Eq. (12))
ξ, ψ, ζ	Coefficient subscript for the approximate expression (Eq. (14))

Subscripts

btc	Charge of the battery
btd	Output of the battery
cd	Power conditioner
cro	Cross-over used by the GA
eq	Optimization analysis of the installed capacity
hex	Amount of supply to the heat network from the SOFC exhaust heat
hp	Heat pump
i	Pieces of equipment that consume electric power

j	Pieces of equipment that consume heat
ls	Value level of a design parameter
m	Number of pieces of power generating equipment
mh	Month
mut	Mutation used by the GA
n	Number of heat equipment
$needs$	Demand
om	Optimization analysis of the operational method
pc	Power conditioner
$pefc$	Proton exchange membrane fuel cell
pex	Quantity supplied to the electric-power grid from the solar cell
pl	Number of design parameters
pv	Photovoltaics
r	Multiplier of 2
rm	Reforming system
rad	Heat dissipation
$sofc$	Solid oxide type fuel cell
st	Heat storage tank
we	Water electrolyzer

References

(1)Huang J, Jiang C, Xu R. A review on distributed energy resources and MicroGrid, Renewable and Sustainable Energy Reviews 2008;12(9);2472-2483.

(2)David VS, Gregory AK. Scott GB. Life cycle energy and environmental analysis of a microgrid power pavilion, Int J Energy Research 2007;31(1);1–13.

(3) Anastasopoulos MP, Voulkidis AC, Athanasios V, Vasilakos PGC. A secure network management protocol for SmartGrid BPL networks: Design, implementation and experimental results, Computer Communications 2008;31(18);4333-4342.

(4)Afzal SS, Chris M, Distributed generation investment by a microgrid under uncertainty, Energy 2008;33(12);1729-1737.

(5) Nirmal-Kumar CNN, Lixi Z. SmartGrid: Future networks for New Zealand power systems incorporating distributed generation, Energy Policy 2009;37(9);3418-3427.

(6) Jingwei C, Youjun L Liejin G, Ximin Z, Peng Xiao. Hydrogen production by biomass gasification in supercritical water using concentrated solar energy: System development and proof of concept. Int J Hydrogen Energy, 35(13)(2010), 7134-7141.

(7) Ryan H. How Green Is the Smart Grid?, The Electricity Journal 2009;22(3);29-41.

(8) Mehrdad SN, Mahmood RH. Multiobjective electric distribution system expansion planning using hybrid energy hub concept, Electric Power Systems Research 2009;79(6);899-911.
(9) Zhenzhong Y, Lijun W, Shilei L. Investigation into the optimization control technique of hydrogen-fueled engines based on genetic algorithms, Int J Hydrogen Energy 2008;33(22);6780-6791.
(10) Garyfallos G, Athanasios IP, Panos SV. Optimum design and operation under uncertainty of power systems using renewable energy sources and hydrogen storage, Int J Hydrogen Energy 2010;35(3);872-891.
(11) Mehrdad SN, Mahmood RH. Multiobjective electric distribution system expansion planning using hybrid energy hub concept, Electric Power Systems Research 2009;79(6);899-911.
(12) Zhenzhong Y, Lijun W, Shilei L. Investigation into the optimization control technique of hydrogen-fueled engines based on genetic algorithms, Int J Hydrogen Energy 2008;33(22);6780-6791.
(13) Garyfallos G, Athanasios IP, Panos S, Spyros V. Optimum design and operation under uncertainty of power systems using renewable energy sources and hydrogen storage, Int J Hydrogen Energy 2010;35(3);872-891.
(14) Li-jun W, Man-lou H, Zhen-zhong Y. Research on optimal calibration technology for hydrogen-fueled engine based on nonlinear programming theory, Int J Hydrogen Energy 2010;35(7);2747-2753.
(15) Lin CY, Lay CH. Effects of carbonate and phosphate concentrations on hydrogen production using anaerobic sewage sludge microflora, Int J Hydrogen Energy 2004;29(3); 275-281.
(16) Wei-Lung Y, Sheng-Ju W, Sheau-Wen S. Parametric analysis of the proton exchange membrane fuel cell performance using design of experiments, Int J Hydrogen Energy 2008;33(9);2311-2322.
(17) Roberto CD, José LE, Vicente M. Thomas Theuss, Juan de Dios Calderón, Omar Solorza, Rubén Rivera, Fractional factorial design of experiments for PEM fuel cell performances improvement, Int J Hydrogen Energy 2003;28(3);343-348.
(18) Narita K. The research on unused energy of the cold region city and utilization for the district heat and cooling, Ph. D. thesis, Hokkaido University, Sapporo; 1996.

Captions

Fig. 1　Independent microgrid with a cascade fuel cell system, photovoltaics, a heat pump, heat storage, and power storage equipment

Fig. 2　Steam reforming system

Fig. 3　Performance of the SOFC and PEFC with the reformer, and COP of the heat pump system

Fig. 4　Chromosome model using the GA

Fig. 5　Analysis flow using the simple GA method

Fig. 6　Analysis flow using the conventional GA method

Fig. 7　Factorial effect chart

Fig. 8　Energy demand pattern and metrological data

Fig. 9　Analysis results of the orthogonal array and the factorial effect chart

Fig. 10　Analysis results of the orthogonal array-GA hybrid method

Fig. 11　Results from the operational analysis

Fig. 12　Results from the optimum analysis of an independent microgrid

Table 1　L_{18} orthogonal array

Table 2　Level of each design parameter

Table 3　Level of each design parameter for the equipment capacity

Table 4　Efficiency of each piece of equipment

Table 5　Unit price for set up

Table 6　Average values of the facility cost and the fuel charge for ten years for every level

(a) The minimum cost for every level of each design parameter

(b) Determining the level for each design parameter

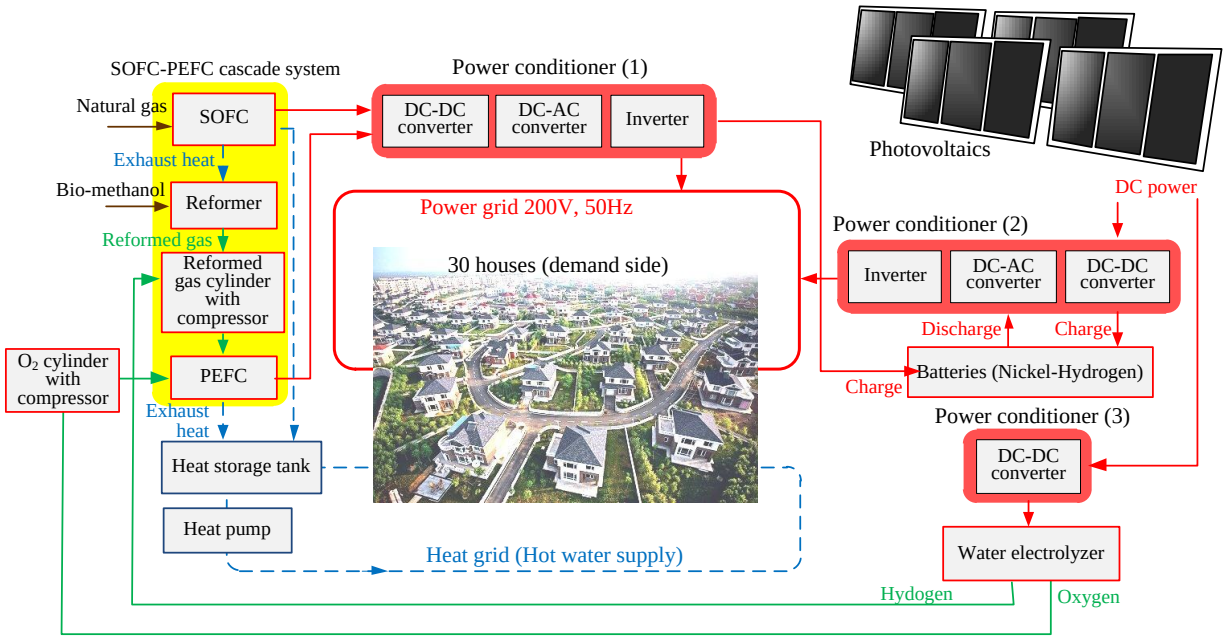

Fig. 1 Independent microgrid with a cascade fuel cell system, photovoltaics, heat pump, a heat storage and power storage equipment

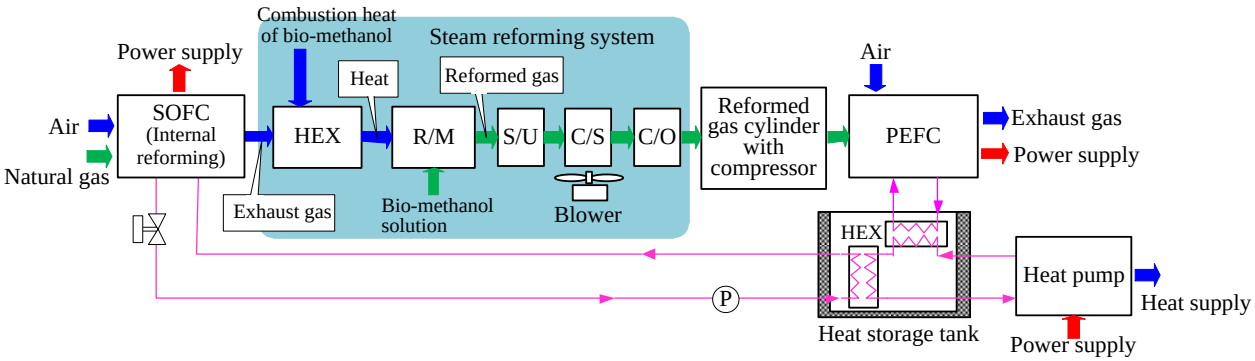

C/O : CO oxidation unit, C/S : Condenser unit, HEX : Heat exchanger, R/M : Reformer, S/U : Shift unit

Fig. 2 Steam reforming system

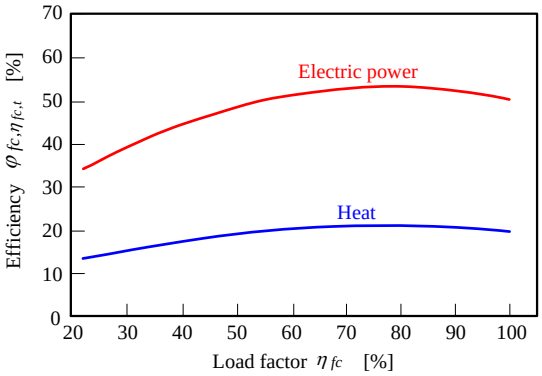

(a) SOFC

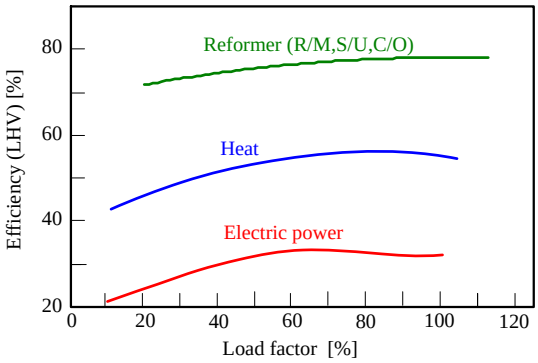

(b) PEFC with steam reformer and reformer

Fig. 3 Performance of the SOFC and PEFC with the reformer

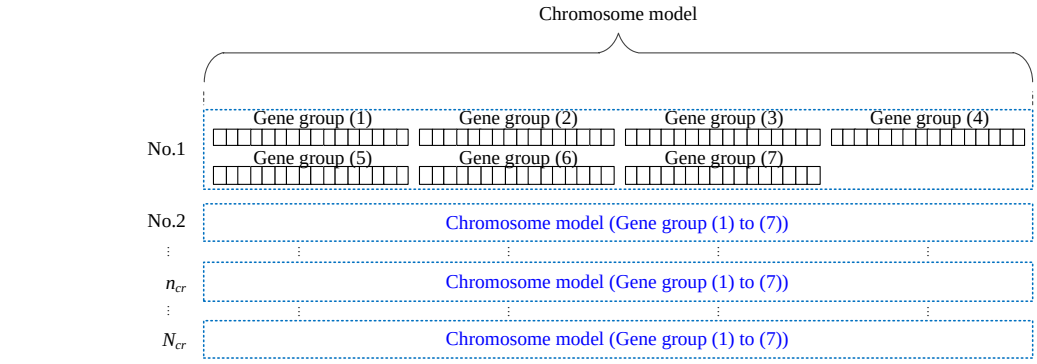

(a) Capacity of equipment

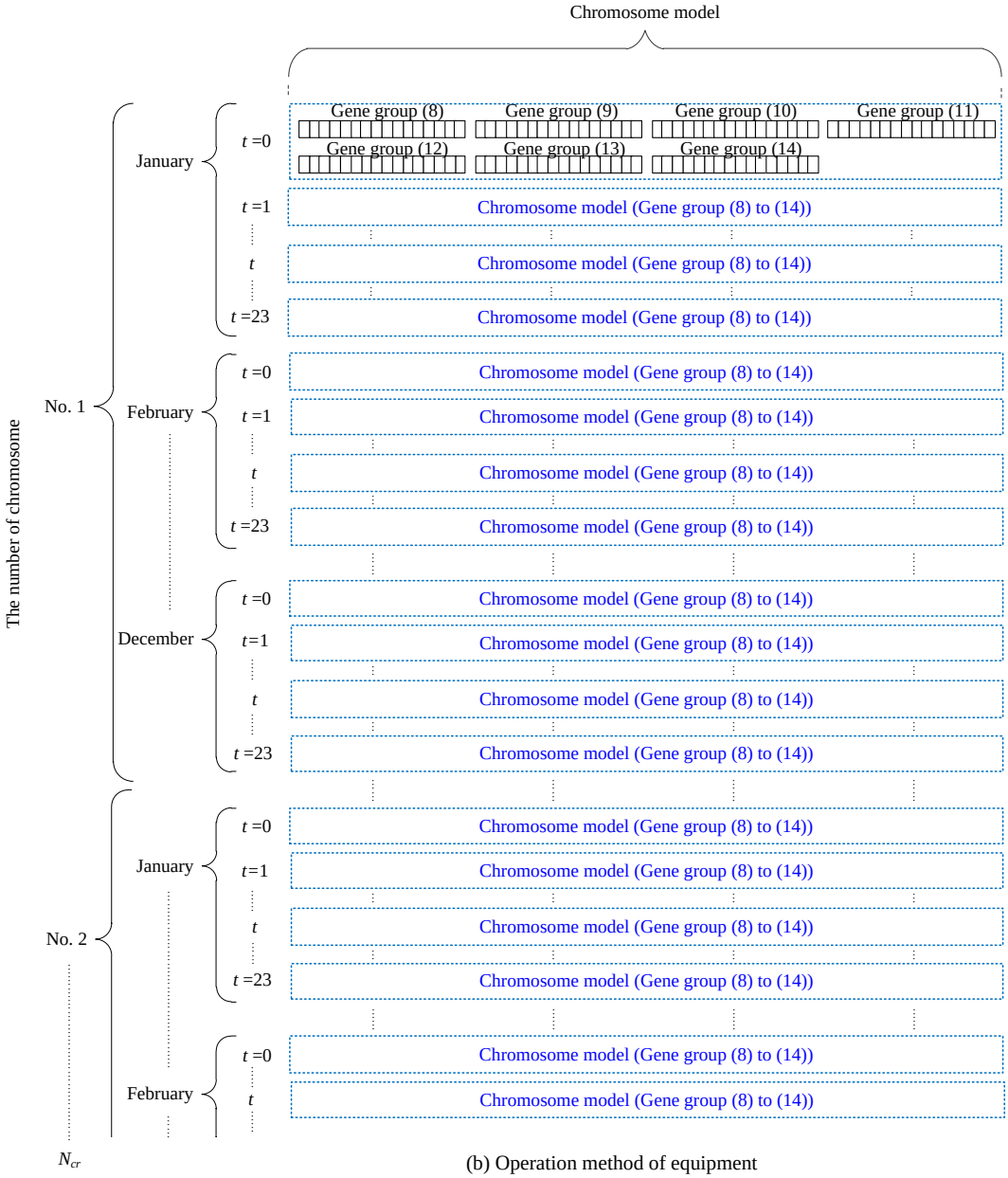

(b) Operation method of equipment

Fig. 4 Chromosome model using the GA

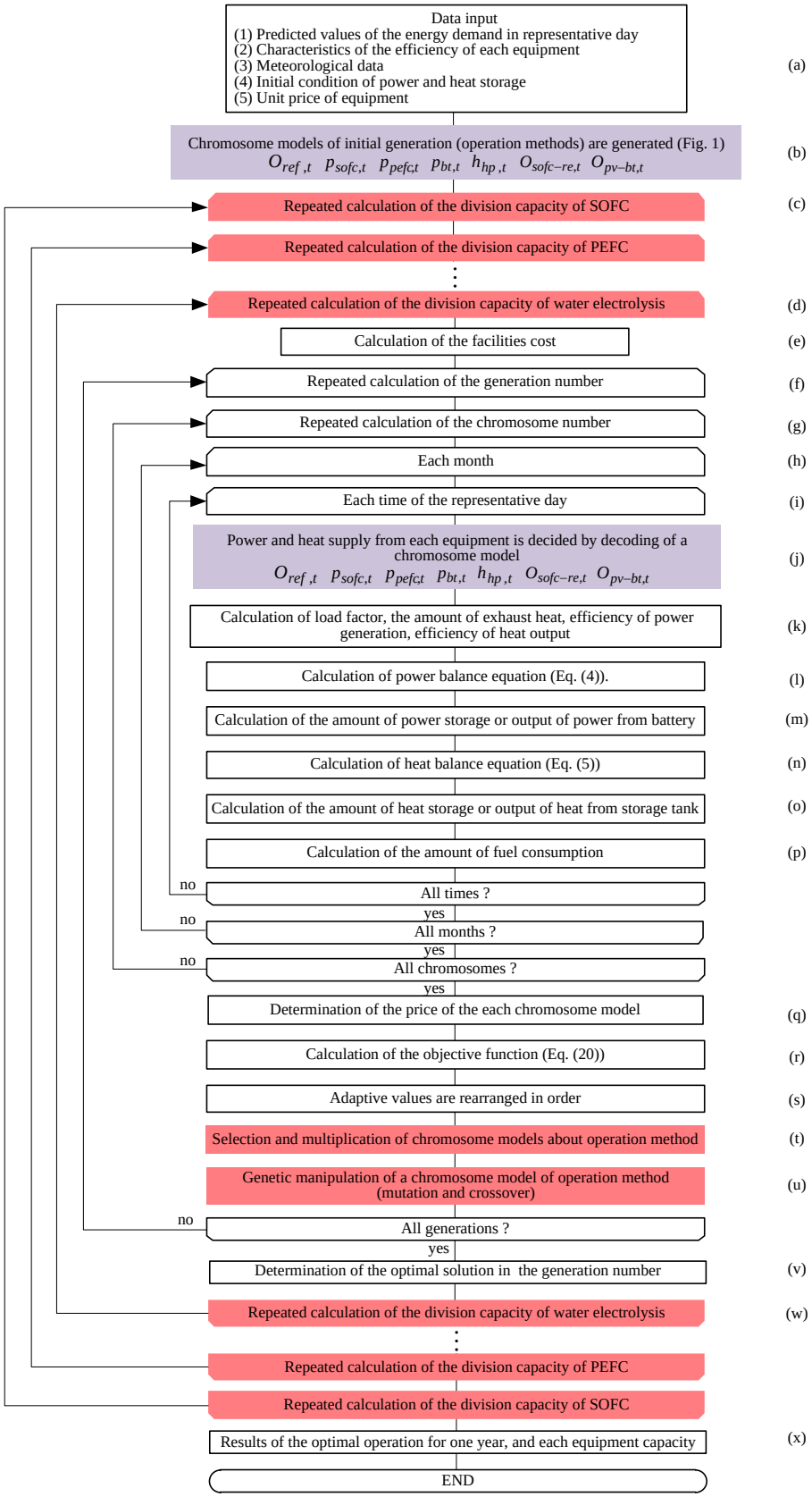

Fig. 5 Analysis flow using the conventional GA method

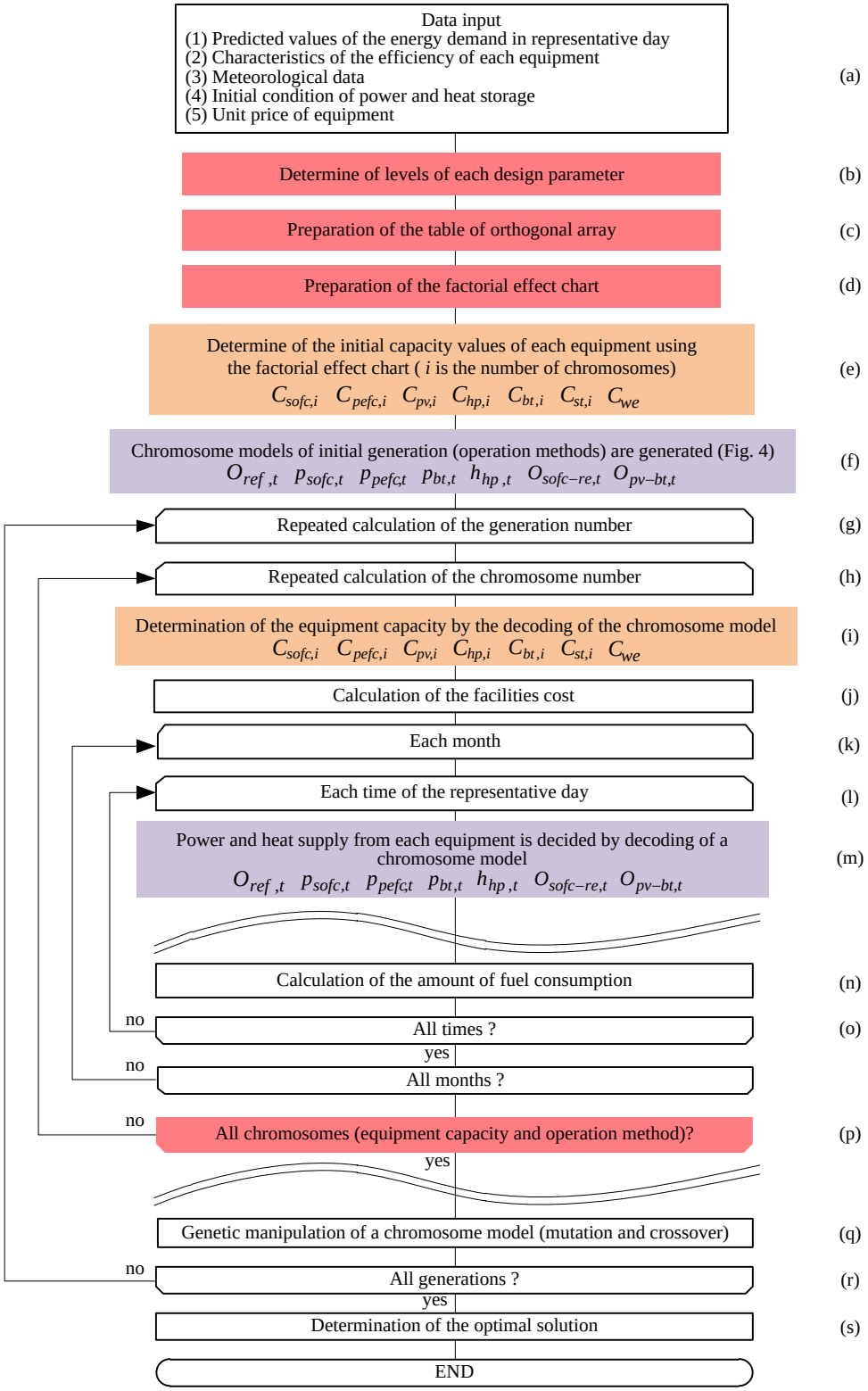

Fig. 6 Analysis flow of the orthogonal array-GA hybrid method (the proposed method)

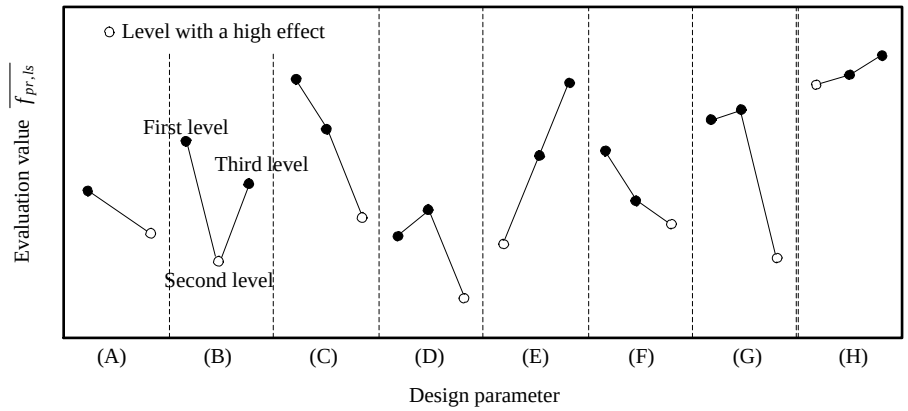

Fig. 7 Factorial effect chart

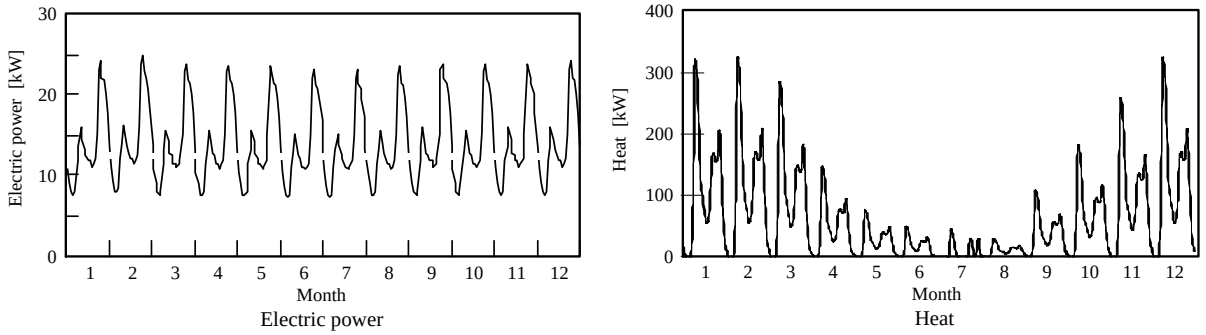

(a) Energy demand pattern (30 houses in Sapporo, Japan)

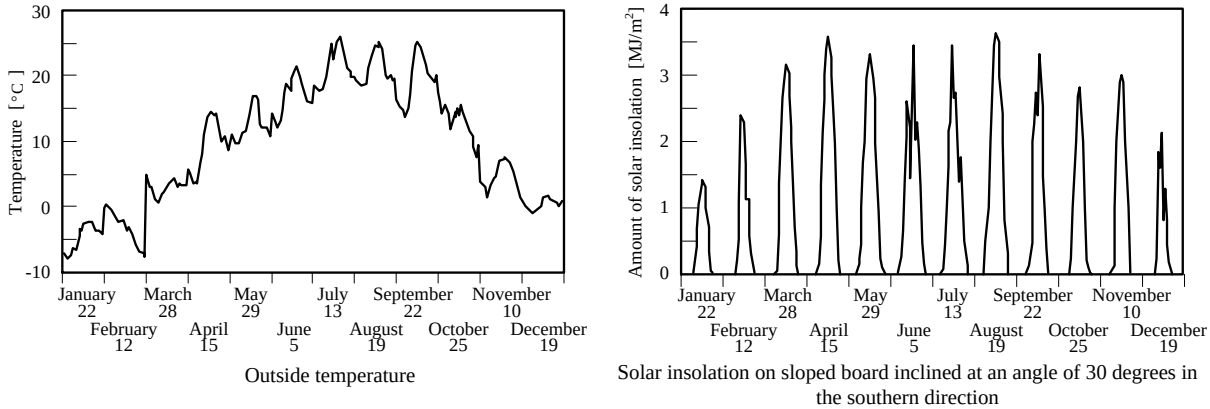

(b) Metrological data

Fig. 8 Energy demand pattern and metrological data

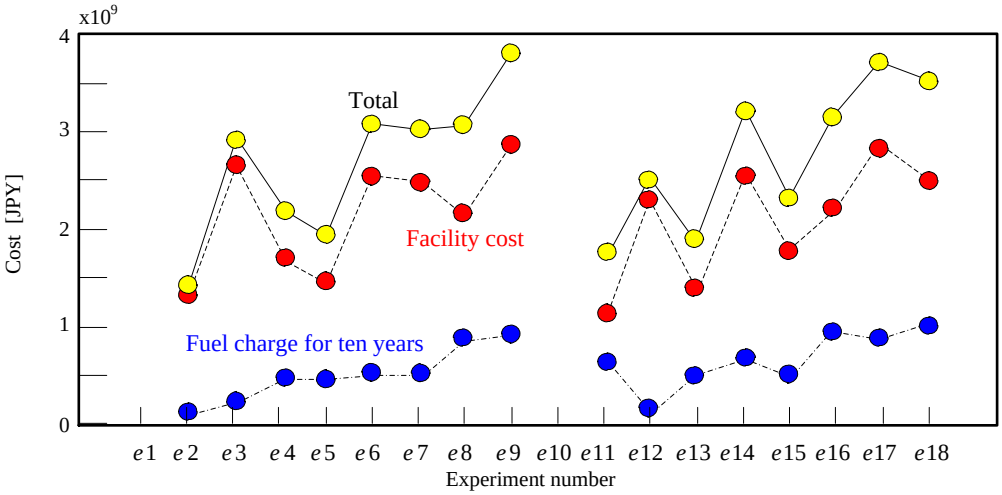

(a) Cost based on the orthogonal array of L_{18}

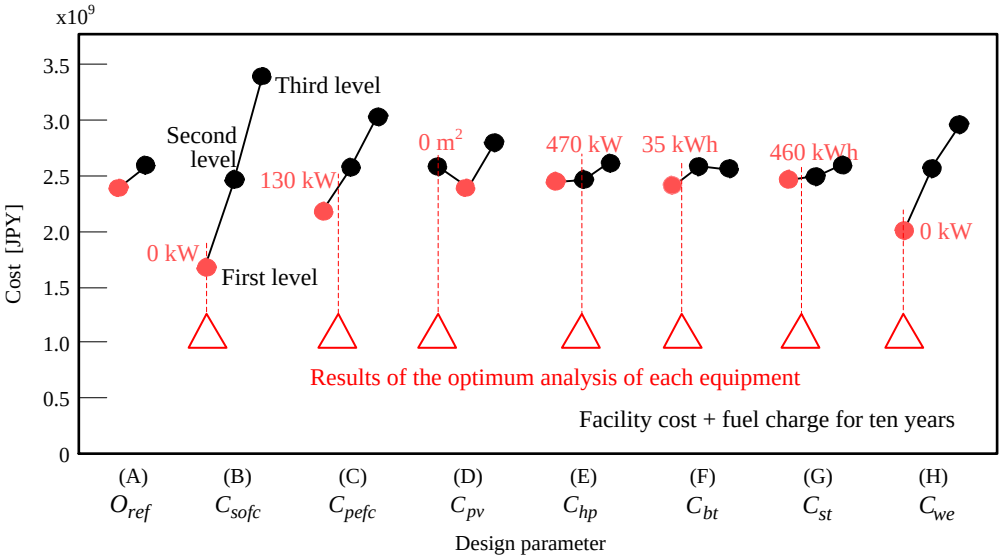

(b) Factorial effect chart

Fig. 9 Analysis results of the orthogonal array and the factorial effect chart

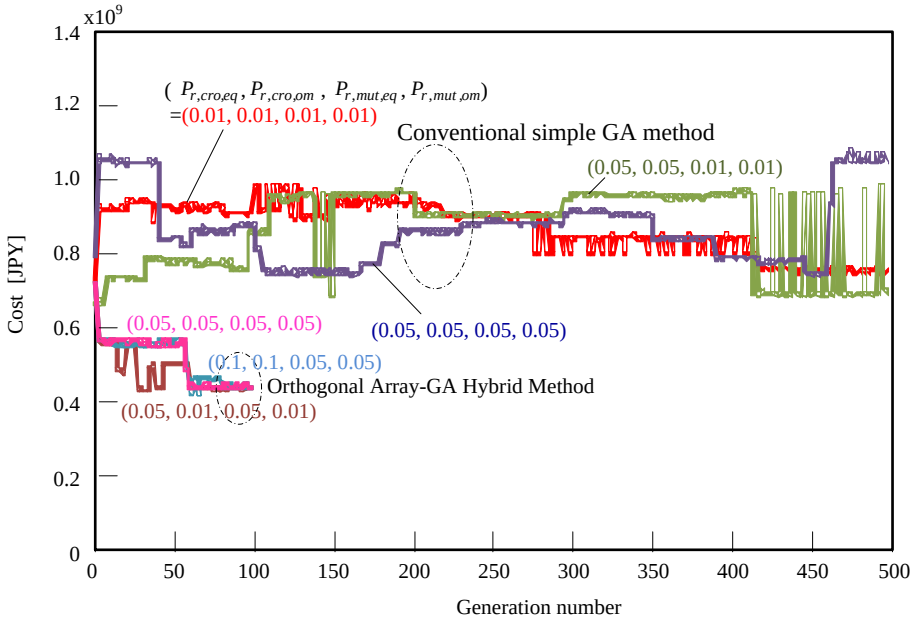

(a) Generation number and cost

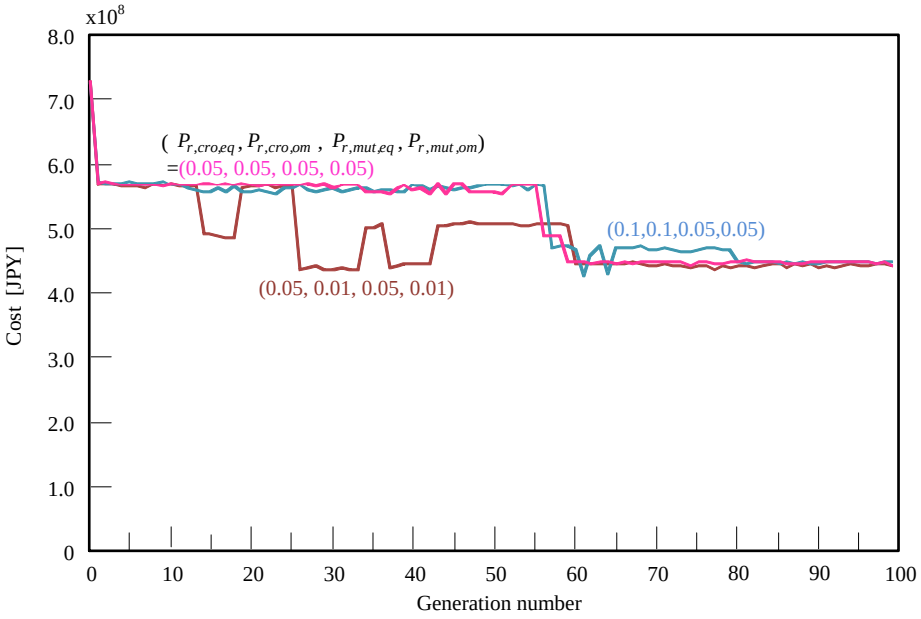

(b) Generation number and cost Using the orthogonal array-GA hybrid method

Fig. 10 Analysis results of the orthogonal array-GA hybrid method

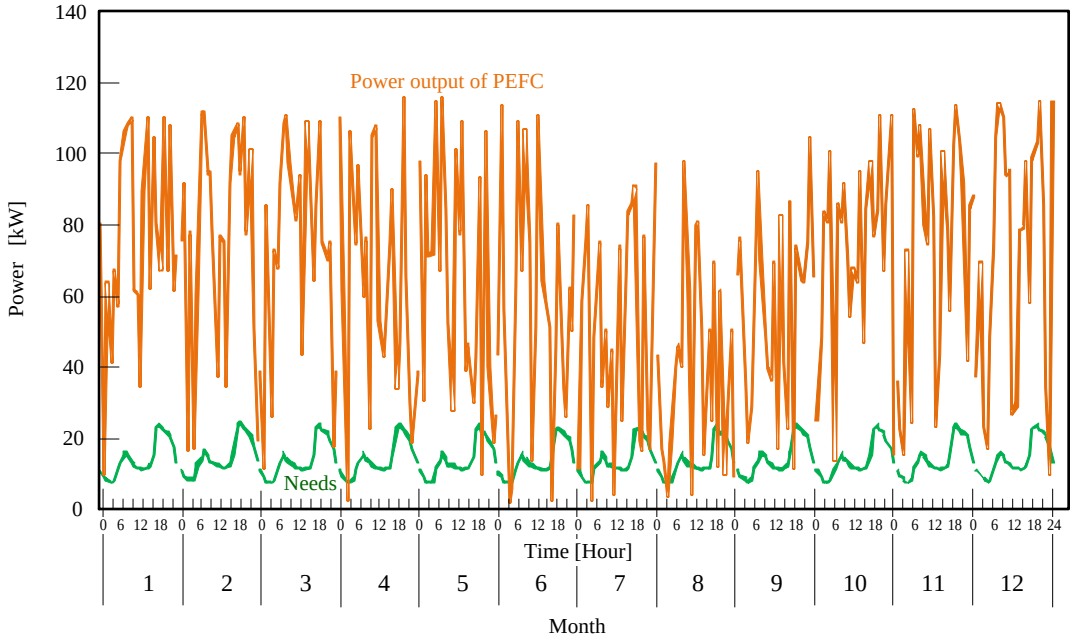

(a) PEFC

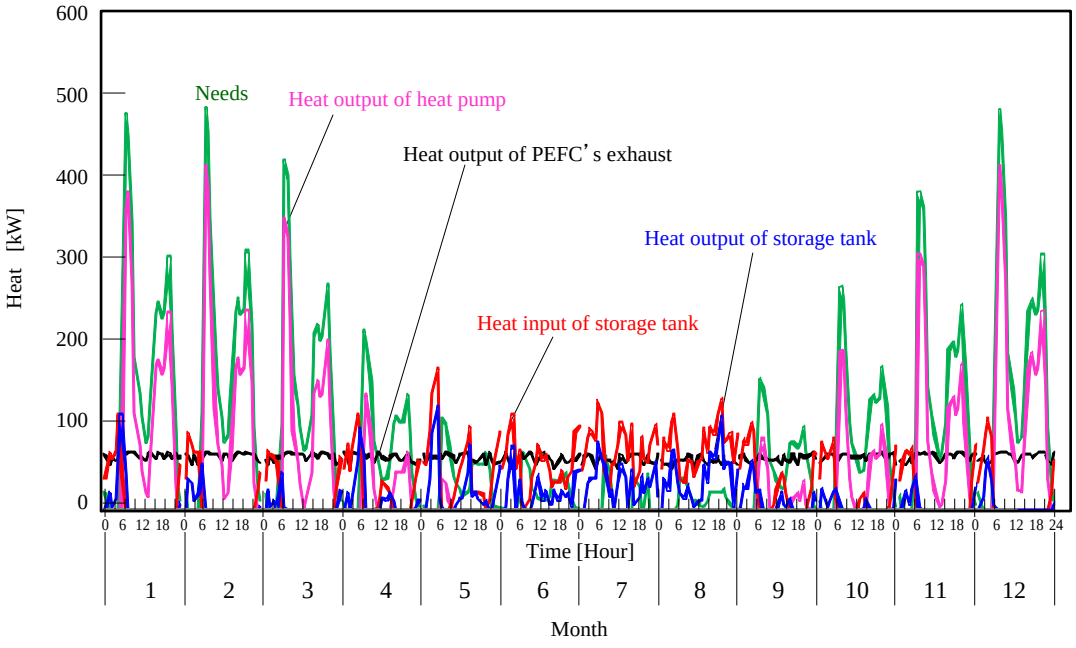

(b) Heat equipment

Fig. 11 Results from the operational analysis

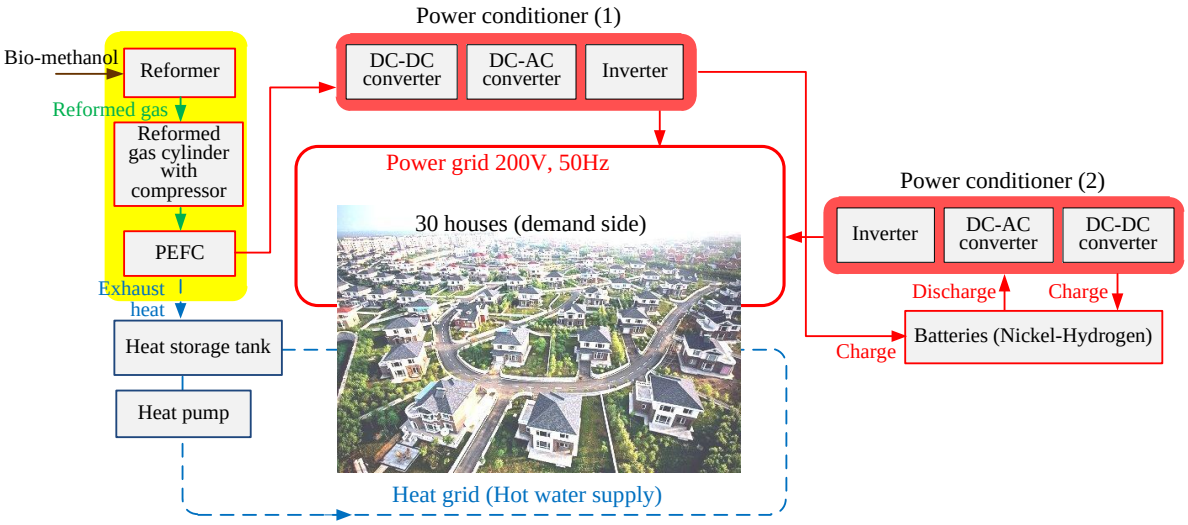

Fig. 12 Results from the optimum analysis of an independent microgrid

Table 1 L_{18} orthogonal array

Experiment number		Row number (Design parameter)								Calculation results of cost					
										Fuel consumptoion				Facilities	Total
		(A)	(B)	(C)	(D)	(E)	(F)	(G)	(H)	t_0	t_1	·····	t_{23}		
	$e1$	1	1	1	1	1	1	1	1	$f_{e1,m,t0}$	$f_{e1,m,t1}$	·····	$f_{e1,m,t23}$	P_{e1}	$y_n \cdot \sum_{m=1}^{12}\sum_{t=0}^{23} f_{e1,m,t} + P_{e1}$
	$e2$	1	1	2	2	2	2	2	2	$f_{e2,m,t0}$	$f_{e2,m,t1}$	·····	$f_{e2,m,t23}$	P_{e2}	$y_n \cdot \sum_{m=1}^{12}\sum_{t=0}^{23} f_{e2,m,t} + P_{e2}$
	$e3$	1	1	3	3	3	3	3	3	$f_{e3,m,t0}$	$f_{e3,m,t1}$	·····	$f_{e3,m,t23}$	P_{e3}	$y_n \cdot \sum_{m=1}^{12}\sum_{t=0}^{23} f_{e3,m,t} + P_{e3}$
	$e4$	1	2	1	1	2	2	3	3	$f_{e4,m,t0}$	$f_{e4,m,t1}$	·····	$f_{e4,m,t23}$	P_{e4}	$y_n \cdot \sum_{m=1}^{12}\sum_{t=0}^{23} f_{e4,m,t} + P_{e4}$
	$e5$	1	2	2	2	3	3	1	1	$f_{e5,m,t0}$	$f_{e5,m,t1}$	·····	$f_{e5,m,t23}$	P_{e5}	$y_n \cdot \sum_{m=1}^{23}\sum_{t=1}^{24} f_{e5,m,t} + P_{e5}$
	$e6$	1	2	3	3	1	1	2	2	$f_{e6,m,t0}$	$f_{e6,m,t1}$	·····	$f_{e6,m,t23}$	P_{e6}	$y_n \cdot \sum_{m=1}^{12}\sum_{t=0}^{23} f_{e6,m,t} + P_{e6}$
	$e7$	1	3	1	2	1	3	2	3	$f_{e7,m,t0}$	$f_{e7,m,t1}$	·····	$f_{e7,m,t23}$	P_{e7}	$y_n \cdot \sum_{m=1}^{12}\sum_{t=0}^{23} f_{e7,m,t} + P_{e7}$
	$e8$	1	3	2	3	2	1	3	1	$f_{e8,m,t0}$	$f_{e8,m,t1}$	·····	$f_{e8,m,t23}$	P_{e8}	$y_n \cdot \sum_{m=1}^{12}\sum_{t=0}^{23} f_{e8,m,t} + P_{e8}$
	$e9$	1	3	3	1	3	2	1	2	$f_{e9,m,t0}$	$f_{e9,m,t1}$	·····	$f_{e9,m,t23}$	P_{e9}	$y_n \cdot \sum_{m=1}^{12}\sum_{t=0}^{23} f_{e9,m,t} + P_{e9}$
	$e10$	2	1	1	3	3	2	2	1	$f_{e10,m,t0}$	$f_{e10,m,t1}$	·····	$f_{e10,m,t23}$	P_{e10}	$y_n \cdot \sum_{m=1}^{12}\sum_{t=0}^{23} f_{e10,m,t} + P_{e10}$
	$e11$	2	1	2	1	1	3	3	2	$f_{e11,m,t0}$	$f_{e11,m,t1}$	·····	$f_{e11,m,t23}$	P_{e11}	$y_n \cdot \sum_{m=1}^{12}\sum_{t=0}^{23} f_{e11,m,t} + P_{e11}$
	$e12$	2	1	3	2	2	1	1	3	$f_{e12,m,t0}$	$f_{e12,m,t1}$	·····	$f_{e12,m,t23}$	P_{e12}	$y_n \cdot \sum_{m=1}^{12}\sum_{t=0}^{23} f_{e12,m,t} + P_{e12}$
	$e13$	2	2	1	2	3	1	3	2	$f_{e13,m,t0}$	$f_{e13,m,t1}$	·····	$f_{e13,m,t23}$	P_{e13}	$y_n \cdot \sum_{m=1}^{12}\sum_{t=0}^{23} f_{e13,m,t} + P_{e13}$
	$e14$	2	2	2	3	1	2	1	3	$f_{e14,m,t0}$	$f_{e14,m,t1}$	·····	$f_{e14,m,t23}$	P_{e14}	$y_n \cdot \sum_{m=1}^{12}\sum_{t=0}^{23} f_{e14,m,t} + P_{e14}$
	$e15$	2	2	3	1	2	3	2	1	$f_{e15,m,t0}$	$f_{e15,m,t1}$	·····	$f_{e15,m,t23}$	P_{e15}	$y_n \cdot \sum_{m=1}^{12}\sum_{t=0}^{23} f_{e15,m,t} + P_{e15}$
	$e16$	2	3	1	3	2	3	1	2	$f_{e16,m,t0}$	$f_{e16,m,t1}$	·····	$f_{e16,m,t23}$	P_{e16}	$y_n \cdot \sum_{m=1}^{12}\sum_{t=0}^{23} f_{e16,m,t} + P_{e16}$
	$e17$	2	3	2	1	3	1	2	3	$f_{e17,m,t0}$	$f_{e17,m,t1}$	·····	$f_{e17,m,t23}$	P_{e17}	$y_n \cdot \sum_{m=1}^{12}\sum_{t=0}^{23} f_{e17,m,t} + P_{e17}$
	$e18$	2	3	3	2	1	2	3	1	$f_{e18,m,t0}$	$f_{e18,m,t1}$	·····	$f_{e18,m,t23}$	P_{e18}	$y_n \cdot \sum_{m=1}^{12}\sum_{t=0}^{23} f_{e18,m,t} + P_{e18}$

Table 2 Level of each design parameter

Design parameters	First level	Second level	Third level
(A) Parameter 1	$x_{p1,1}$	$x_{p1,2}$	
(B) Parameter 2	$x_{p2,1}$	$x_{p2,2}$	$x_{p2,3}$
(C) Parameter 3	$x_{p3,1}$	$x_{p3,2}$	$x_{p3,3}$
(D) Parameter 4	$x_{p4,1}$	$x_{p4,2}$	$x_{p4,3}$
(E) Parameter 5	$x_{p5,1}$	$x_{p5,2}$	$x_{p5,3}$
(F) Parameter 6	$x_{p6,1}$	$x_{p6,2}$	$x_{p6,3}$
(G) Parameter 7	$x_{p7,1}$	$x_{p7,2}$	$x_{p7,3}$
(H) Parameter 8	$x_{p8,1}$	$x_{p8,2}$	$x_{p8,3}$

Table 3 Level of each design parameter for the equipment capacity

Design parameters of equipment capacity	First level	Second level	Third level
(A) Changeover switch of the output of solar cell δ	0 (Battery)	1 (Water electrolysis)	
(B) Capacity of SOFC [kW] C_{sofc}	0	250	500
(C) Capacity of PEFC [kW] C_{pefc}	0	250	500
(D) Capacity of Photovoltaics [m²] C_{pv}	0	1000	2000
(E) Capacity of heat pump [kW] C_{hp}	0	500	1000
(F) Capacity of battery [kWh] C_{bt}	0	100	200
(G) Capacity of heat storage tank [kWh] C_{st}	0	1000	2000
(H) Capacity of water electrolysis [kW] C_{we}	0	250	500

Table 4 Efficiency of each piece of equipment

Solar cell (with power conditioner):	0.18
Heat storage tank:	0.8
Battery (efficiency of charge and discharge):	0.9
Power conditioner using SOFC:	0.9
Power transmission of power grid:	1.0
Heat supply to heat grid:	1.0

Table 5 Unit price for set up

Japanese yen (1 USD=78 JPY)

SOFC	2,500,000 JPY/kW
PEFC	2,000,000 JPY/kW
Photovoltaics	82,200 JPY/kW
Heat pump	100,000 JPY/kW
Battery	450,000 JPY/kWh
Heat storage tank	10,000 JPY/kWh
Water electrolysis	2,000,000 JPY/kW
Cylinders (two)	1,000 JPY/kWh
Compressor (two)	20,000 JPY/kW
Power conditioner	110,000 JPY/kW
Reformer system	500,000 JPY/kW

Table 6 Average values of the facility cost and the fuel charge for ten years for every level

(a) The minimum cost for every level of each design parameter

$x10^9$ [JPY]

	First level	Second level	Third level
(A)	$2.40X10^9$	$2.61X10^9$	
(B)	$1.65X10^9$	$2.46X10^9$	$3.39X10^9$
(C)	$2.17X10^9$	$2.56X10^9$	$3.03X10^9$
(D)	$2.57X10^9$	$2.40X10^9$	$2.79X10^9$
(E)	$2.45X10^9$	$2.46X10^9$	$2.60X10^9$
(F)	$2.39X10^9$	$2.58X10^9$	$2.54X10^9$
(G)	$2.46X10^9$	$2.47X10^9$	$2.58X10^9$
(H)	$2.02X10^9$	$2.55X10^9$	$2.94X10^9$

(b) Determining the level for each design parameter

$x10^9$ [JPY]

	First level	Second level	Third level
(A)	$2.40X10^9$	$2.61X10^9$	
(B)	$1.65X10^9$	$2.46X10^9$	$3.39X10^9$
(C)	$2.17X10^9$	**$2.56X10^9$**	$3.03X10^9$
(D)	**$2.57X10^9$**	$2.40X10^9$	$2.79X10^9$
(E)	$2.45X10^9$	**$2.46X10^9$**	$2.60X10^9$
(F)	$2.39X10^9$	$2.58X10^9$	$2.54X10^9$
(G)	$2.46X10^9$	**$2.47X10^9$**	$2.58X10^9$
(H)	$2.02X10^9$	$2.55X10^9$	$2.94X10^9$